Int. J. Solids Structures Vol. 28, No. 2, pp. 235–248, 1991
Printed in Great Britain.

0020–7683/91 $3.00 + .00
Pergamon Press plc

ORTHOTROPY RESCALING AND IMPLICATIONS FOR FRACTURE IN COMPOSITES

Z. SUO
Department of Mechanical Engineering and Environmental Engineering,
University of California, Santa Barbara, CA 93106, U.S.A.

G. BAO and B. FAN
Materials Department, University of California, Santa Barbara, CA 93106, U.S.A.

and

T. C. WANG
Institute of Mechanics, Chinese Academy of Sciences, Beijing 100080, P.R.C.

(*Received* 8 *May* 1990; *in revised form* 9 *November* 1990)

Abstract—For most practically important plane elasticity problems of orthotropic materials, stresses depend on elastic constants through two nondimensional combinations. A spatial rescaling has been found to reduce the orthotropic problems to equivalent problems in materials with cubic symmetry. The latter, under favorable conditions, may be approximated by isotropic materials. Consequently, solutions for orthotropic materials can be constructed approximately from isotropic material solutions or rigorously from cubic ones. The concept is developed to gain insight into the interplay between anisotropy and finite geometry. The inherent simplicity of the solutions allows a variety of technical problems to be addressed efficiently. Included are stress concentration related cracking, effective contraction of orthotropic material specimens, crack deflection onto easy fracture planes, and surface flaw induced delamination.

1. INTRODUCTION

Various advanced composite material concepts have been explored in recent years. Composites are fabricated using ceramics, intermetallics, metals and polymers, with a variety of configurations: fiber, whisker, particle and plate reinforcements, laminates and multilayers, etc. These materials, together with other examples such as woods and oriented polymers, exhibit failure behaviors that are governed by anisotropic and heterogeneous characteristics (Ashby *et al.*, 1985; Evans, 1990; O'Brien, 1987; Sweeney *et al.*, 1988). An adequate assessment of the mechanical properties of these materials requires experiments that identify failure progressions and micromechanic models that quantify them. Mechanics solutions for flaw-containing geometries with anisotropic and heterogeneous features are usually involved in both aspects of the investigations.

In a recent paper (Suo, 1990a), a spatial rescaling was found to reduce plane elasticity problems for orthotropic materials to equivalent problems for materials with cubic symmetry. Practically, the latter may be approximated by isotropic ones under favorable conditions. The concept thus provides a *routine procedure* to extract approximate solutions for orthotropic materials, without any work, from isotropic solutions in standard handbooks, such as those of stress intensity factors (Tada *et al.*, 1985) and stress concentration factors (Peterson, 1974). The concept is further developed here to study several important technical problems, including cracks emanating from holes, fracture specimens, delamination and crack deflection. Insight is gained into the interplay of anisotropy and finite geometry that has long been puzzling. Moreover, the rescaling significantly reduces the effort to compile analytic and numerical solutions for various practically important geometries. A comprehensive finite element study on an array of commonly used fracture specimens for composites and woods is in progress. A user-friendly catalog of specimen calibrations has emerged as being guided by the orthotropy rescaling, which will be reported in a separate work (Bao *et al.*, 1991).

2. ORTHOTROPY RESCALING

Plane stress states in a principal plane of an orthotropic solid will be assumed in the body of the text. The procedure to obtain the corresponding solutions under plane strain conditions is described in the Appendix. The coordinates x and y coincide with the principal axes 1 and 2, respectively. Following Suo (1990a,b), we define two nondimensional elastic parameters

$$\lambda = \frac{s_{11}}{s_{22}}, \quad \rho = \frac{2s_{12}+s_{66}}{2\sqrt{s_{11}s_{22}}}. \tag{1}$$

Here s_{ij} are compliances as defined in the Appendix, which correspond to the Young's and shear moduli and Poisson's ratios

$$s_{11} = \frac{1}{E_1}, \quad s_{22} = \frac{1}{E_2}, \quad s_{66} = \frac{1}{G_{12}}, \quad s_{12} = -\frac{\nu_{12}}{E_1} = -\frac{\nu_{21}}{E_2}. \tag{2}$$

In terms of these engineering quantities, the following two dimensionless numbers can be expressed

$$\lambda = \frac{E_2}{E_1}, \quad \rho = \frac{(E_1E_2)^{1/2}}{2G_{12}} - (\nu_{12}\nu_{21})^{1/2}. \tag{3}$$

The parameters measure the in-plane orthotropy: $\lambda = \rho = 1$ for isotropic solids and $\lambda = 1$ for solids with cubic symmetry. It turns out that a class of hypothetical materials obeying $\rho = 1$ but $\lambda \neq 1$ play an important role in the conceptual development. Such materials will be called *degenerate orthotropic* for reasons that will become clear later. The requirement of positive energy density for all strain states implies that $\lambda > 0$ and $\rho > -1$. Values for representative woods and composites are in the range $0.05 < \lambda < 20$ and $0 < \rho < 5$.

Let $U(x, y)$ be the Airy stress function so that stresses at equilibrium can be expressed by

$$\sigma_x = \frac{\partial^2 U}{\partial y^2}, \quad \sigma_y = \frac{\partial^2 U}{\partial x^2}, \quad \tau_{xy} = -\frac{\partial^2 U}{\partial x\,\partial y}. \tag{4}$$

In addition, the compatibility implies (Lekhnitskii, 1981)

$$\frac{\partial^4 U}{\partial x^4} + 2\rho\lambda^{1/2}\frac{\partial^4 U}{\partial x^2\,\partial y^2} + \lambda\frac{\partial^4 U}{\partial y^4} = 0. \tag{5}$$

The above equations suggest that stresses depend on material properties only through λ and ρ in simply-connected sheets with traction prescribed on the boundary. Further, the rescaling described below allows the λ dependence to be extracted explicitly.

Rescale the x-axis by

$$\xi = \lambda^{1/4}x, \tag{6}$$

and the governing equation (5) now exhibits ρ dependence only

$$\frac{\partial^4 U}{\partial \xi^4} + 2\rho\frac{\partial^4 U}{\partial \xi^2\,\partial y^2} + \frac{\partial^4 U}{\partial y^4} = 0. \tag{7}$$

Boundary conditions for U are rescaled accordingly

$$\sigma_x = \frac{\partial^2 U}{\partial y^2}, \quad \lambda^{-1/2}\sigma_y = \frac{\partial^2 U}{\partial \xi^2}, \quad \lambda^{-1/4}\tau_{xy} = -\frac{\partial^2 U}{\partial \xi\, \partial y}. \tag{8}$$

With λ absorbed in loading and geometric parameters, the boundary value problems on the ξy-plane have only one material constant, ρ, as in the governing equation (7). Observe that for the degenerate materials with $\rho = 1$, the governing equation is identical to that for isotropic materials. Consequently, solutions to degenerate orthotropic materials can be readily constructed from those to isotropic ones. The detailed procedure will be illustrated in the following sections.

For a crack in the x-direction, the stress intensity factors are defined such that

$$K_{\mathrm{I}} \sim (2\pi x)^{1/2}\sigma_y, \quad K_{\mathrm{II}} \sim (2\pi x)^{1/2}\tau_{xy} \tag{9}$$

where σ_y and τ_{xy} are tractions a distance x ahead of the crack tip. On the ξy-plane, the above can be written as

$$\lambda^{-3/8}K_{\mathrm{I}} \sim (2\pi\xi)^{1/2}\frac{\partial^2 U}{\partial \xi^2}, \quad \lambda^{-1/8}K_{\mathrm{II}} \sim -(2\pi\xi)^{1/2}\frac{\partial^2 U}{\partial \xi\, \partial y}. \tag{10}$$

Stress intensity factors for a crack running in the y-direction are defined analogously to scale σ_x and τ_{xy} directly ahead of the tip, which can be expressed on the ξy-plane

$$K_{\mathrm{I}} \sim (2\pi y)^{1/2}\frac{\partial^2 U}{\partial y^2}, \quad \lambda^{-1/4}K_{\mathrm{II}} \sim -(2\pi y)^{1/2}\frac{\partial^2 U}{\partial \xi\, \partial y}. \tag{11}$$

These expressions are useful in constructing the λ dependence.

To facilitate later studies, we cite the relations between energy release rates associated with the two fracture modes and the stress intensity factors (Sih *et al.*, 1965). For a crack in the x-direction they are

$$G_{\mathrm{I}} = \left(s_{11}s_{22}\frac{1+\rho}{2}\right)^{1/2}\lambda^{-1/4}K_{\mathrm{I}}^2, \quad G_{\mathrm{II}} = \left(s_{11}s_{22}\frac{1+\rho}{2}\right)^{1/2}\lambda^{1/4}K_{\mathrm{II}}^2 \tag{12}$$

and for a crack in the y-direction they are

$$G_{\mathrm{I}} = \left(s_{11}s_{22}\frac{1+\rho}{2}\right)^{1/2}\lambda^{1/4}K_{\mathrm{I}}^2, \quad G_{\mathrm{II}} = \left(s_{11}s_{22}\frac{1+\rho}{2}\right)^{1/2}\lambda^{-1/4}K_{\mathrm{II}}^2. \tag{13}$$

The total energy release rate is $G = G_{\mathrm{I}} + G_{\mathrm{II}}$ for both cases. The above relations establish the equivalence of the stress intensity factors and energy release rates. For a given problem, the one which renders a simpler expression will be chosen to present the solution.

3. CRACKS EMANATING FROM HOLES

Cracks are likely to initiate at stress concentration sites such as holes and corners. Isotropic elasticity solutions for stress concentration/intensity factors for most practical geometries are available in several handbooks. The rescaling allows corresponding solutions for the degenerate orthotropic materials to be constructed without solving new problems. The concept is illustrated with an elliptic hole with and without emanating cracks in an infinite orthotropic sheet subjected to remote tension.

As depicted in Fig. 1, the transformation (6) rescales an ellipse in the xy-plane to a different ellipse in the ξy-plane. Boundary conditions that determine the Airy function U on the ξy-plane are modified according to (8). Linearity and dimensionality dictate that the hoop stress at point A takes the form

$$\sigma_y(A)/\sigma = C(\rho, \lambda^{1/4} b/c). \tag{14}$$

As a consequence of the rescaling, the stress concentration factor $C(\rho, t)$ is a function of two dimensionless variables instead of three. The interplay of the orthotropic parameter λ and aspect ratio b/c can therefore be appreciated even without knowing the actual form of C: the stress concentration factor for the orthotropic sheet is the same for an ellipse with a different aspect ratio, $(\lambda^{1/4} b)/c$, in a cubic sheet.

The stress concentration factor for an elliptic hole in isotropic solids is well known (Peterson, 1974, p. 84)

$$C(1, t) = 1 + 2t. \tag{15}$$

Without solving any new problem, one obtains the stress concentration factor for an elliptic hole in the degenerate orthotropic materials

$$\sigma_y(A)/\sigma = 1 + 2\lambda^{1/4} b/c, \quad \rho = 1. \tag{16}$$

For example, suppose a circular hole ($b = c$) in a composite is loaded in tension in the fiber direction ($\lambda \gg 1$), eqn (16) reveals that orthotropy amplifies the stress concentration: a price must be paid for using composites.

The solution for nondegenerate orthotropic solids requires the complete determination of the function $C(\rho, t)$. Since the second variable, t, can be varied by varying either the aspect ratio b/c or orthotropy λ, the complete problem is solved if *one* of the following problems is solved: (i) a circular hole in an orthotropic material sheet or (ii) an elliptic hole in a cubic material sheet. For this classical problem, both solutions are available in Lekhnitskii (1981), which gives

$$C(\rho, t) = 1 + \sqrt{2}(1+\rho)^{1/2} t. \tag{17}$$

Comparison of (17) with (14) yields the stress concentration factor for an elliptic hole in a generally orthotropic sheet

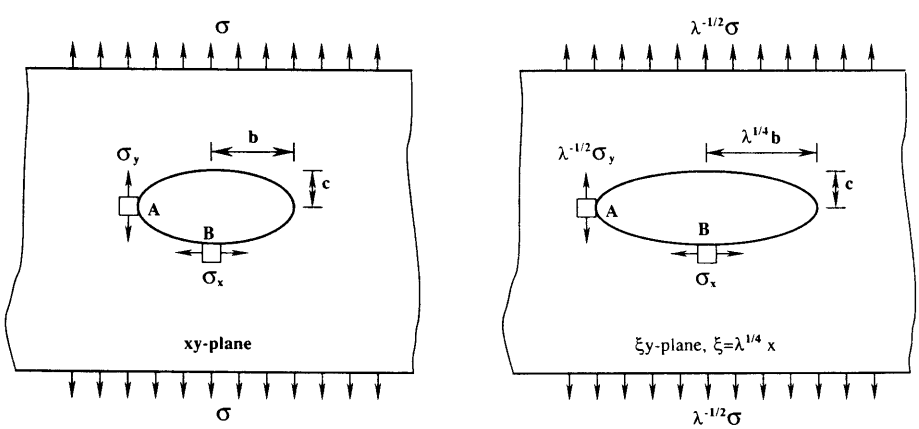

Fig. 1. Orthotropy rescaling. The boundary value problem on the ξy-plane is for a cubic material governed by eqn (7) in the text. The geometry and boundary conditions are rescaled from the original problem on the xy-plane.

$$\sigma_y(A)/\sigma = 1+\sqrt{2}(1+\rho)^{1/2}\lambda^{1/4}b/c. \tag{18}$$

Observe that the ρ dependence is relatively significant for this particular case. Interestingly, similar analysis shows the stress concentration factor at point B in Fig. 1 is ρ-independent

$$\sigma_x(B)/\sigma = -\lambda^{-1/2}. \tag{19}$$

Consider next cracks emanating from an elliptic hole in an orthotropic material subjected to remote tension (Fig. 2). The stress intensity factor chart is reproduced directly from Tada *et al.* (1985, p. 19.8), except for the λ dependence added according to the orthotropy rescaling. With such a slight reinterpretation, the chart is thus valid for degenerate orthotropic materials. For example, the chart gives the results for a circular hole in orthotropic materials when $b = c$.

Formally, the stress intensity factor at an emanating crack tip takes the form

$$K_I = \sigma\sqrt{\pi a}F\left(\frac{a}{a+b}, \lambda^{-1/4}\frac{c}{b}, \rho\right). \tag{20}$$

The plot of Fig. 2 is essentially the function $F(s, t, 1)$. Although the ρ dependence cannot be determined by the rescaling, solutions for limiting cases would be helpful before more complete solutions become available. For example, the stress intensity factor for a crack of length $2d$ in an infinite orthotropic sheet is known to be independent of material properties (Sih *et al.*, 1965)

$$K_I = \sigma\sqrt{\pi d}. \tag{21}$$

Used in an asymptotic sense, this classical solution provides the following information on F

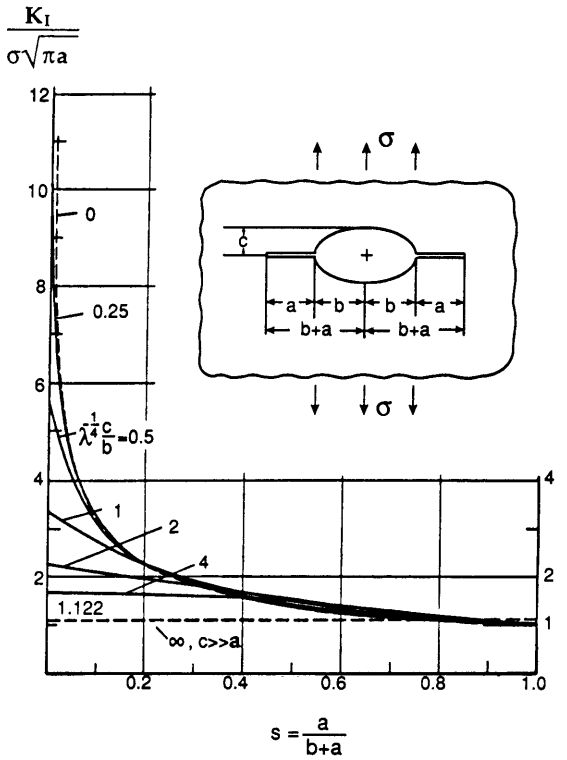

Fig. 2. Stress intensity factors for cracks emanating from an elliptic hole in a degenerate orthotropic material sheet.

$$F(s,0,\rho) = s^{-1/2}, \quad F(1,t,\rho) = 1, \tag{22}$$

suggesting that the ρ-effect should be small for long cracks. The asymptotic solution for *short cracks* can be obtained using the stress intensity factor for an edge crack, with the applied stress amplified by the stress concentration factor (18)

$$K_1 = Y\sigma\sqrt{\pi a}[1+\sqrt{2}(1+\rho)^{1/2}\lambda^{1/4}b/c], \quad Y = 1.12-0.011(\rho-1). \tag{23}$$

Here the function $Y(\rho)$ is the calibration factor for an edge crack in a semi-infinite body; the approximate formula is a linear fit of the numerical results of Sweeney (1988).

In summary, the rescaling allows solutions for degenerate orthotropic materials to be constructed, without solving new problems, from existing solutions for isotropic materials. For situations when ρ is not very different from 1, or the data available do not allow an accurate evaluation of ρ, one may be satisfied with such degenerate solutions which take the principal orthotropy λ *explicitly* into account. Solutions for nondegenerate orthotropic materials require solving new boundary value problems, since there are no general guidelines on the sensitivity of the ρ dependence at this stage. However, only cubic material solutions are needed to construct the full orthotropic solutions. Rescaling in this latter context would contract one variable in the compilation of numerical charts.

4. $\lambda^{1/4}$-CONTRACTION OF FRACTURE SPECIMENS

The compliance calibration is still heavily used in composite material fracture testing for the lack of accurate elasticity solutions. Empirical calibrations obtained in this way should only be valid for the materials being tested, since stresses in orthotropic materials depend on elastic constants. This may partially explain why there are so many different empirical formulae in the literature even for the most basic geometry, such as double-cantilever beams. Guided by the orthotropy rescaling, a comprehensive finite element calculation for a variety of commonly used fracture specimens is in progress, and the results will be reported in Bao *et al.* (1990, 1991). Here a unique feature of anisotropic material specimens will be discussed.

Most fracture specimens for composites are fabricated with strips in the fiber direction, with pre-cracks either normal or parallel to the fibers. In this section the x-axis coincides with the fiber direction so that $\lambda < 1$. Calibrations for infinitely long strips are often adopted in data reduction with the supposition that end-effects would decay rapidly. However, the rescaling reveals that end-zones for orthotropic specimens are $\lambda^{-1/4}$ times their isotropic counterparts. In other words, the effective lengths of the orthotropic specimens are contracted by a factor of $\lambda^{1/4}$. Consequently, longer specimens must be used for orthotropic materials in order to avoid end-effect complications. The phenomenon may be termed as $\lambda^{1/4}$-*contraction*, which is universal whenever orthotropic materials are loaded in a stronger material direction.

To illustrate the concept, consider the double-cantilever beam (DCB) in Fig. 3. Rig-

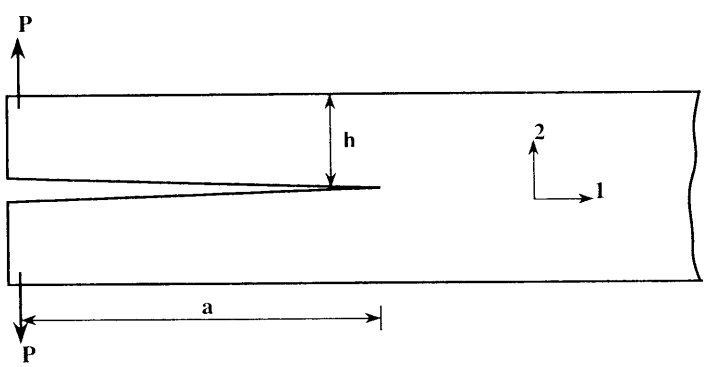

Fig. 3. A double-cantilever beam along the fiber direction. P is the load per unit width of the specimen.

orous analytic considerations show the energy release rate should take the form

$$G = s_{11}(Pa)^2 h^{-3} g(\rho, \lambda^{-1/4} h/a) \tag{24}$$

where P is the applied load per unit width of the strip, and g a nondimensional function of two dimensionless variables, with the rescaling property built in.

The numerical solution for isotropic materials in Wiederhorn *et al.* (1968) gives

$$g(1, t) = 12(1+0.677t)^2. \tag{25}$$

The first term reproduces the result of the elementary beam theory, which is an exact linear elasticity asymptote as the crack length is long compared with the beam thickness. The second term is the correction due to the finite ratio a/h. An independent finite element calculation shows that the error of (25) is within 1% whenever $a/h > 1$. For the degenerate orthotropic materials with $\rho = 1$, combination of eqns (24) and (25) yields

$$G = 12 s_{11}(Pa)^2 h^{-3}(1+0.677\lambda^{-1/4} h/a)^2. \tag{25a}$$

The second term in parentheses is usually omitted in isotropic material testing. The term becomes non-negligible for materials with high orthotropy ($\lambda \ll 1$) unless longer pre-crack is used.

Finite element calculation indicates that the second term is also sensitively dependent on the parameter ρ. The numerical results can be summarized compactly as

$$G = 12 s_{11}(Pa)^2 h^{-3}(1 + Y\lambda^{-1/4} h/a)^2$$
$$Y(\rho) = 0.677 + 0.149(\rho - 1) - 0.013(\rho - 1)^2. \tag{26}$$

This last result is valid for generally orthotropic materials within the entire practical range $\lambda^{1/4} a/h > 1$ and $0 < \rho < 5$, and the error is within 1%.

5. SMALL-SCALE KINKING

For materials that possess planes having lower fracture resistance than other planes, cracks may veer towards such weak planes under favorable conditions. Woods, for example, are relatively strong when loaded along grains; an incipient crack running in from the surface is often deflected along the plane containing grains, setting up cracks at right angles to the original. Other well known examples are cleavage planes in certain crystals, and planes containing fibers in composites. However, it does not follow that cracks will always be deflected whenever such an easy fracture plane exists. Whether a crack will be deflected also depends on the relative driving force available for the potential fracture paths. Several deflection criteria have been discussed in the literature; the present work extends the energetic criterion for elastically isotropic solids such as some ceramic–matrix composites previously proposed by He and Hutchinson (1989).

A parent crack in the x-direction deflected into the y-direction is shown in Fig. 4. A small-scale kinking problem appropriate for the initial deflection is posed: the kink size is much smaller than all other macroscopic in-plane lengths so that the actual specimen geometry and applied load can be represented by the remote nominal stress intensity factors K_I and K_{II}. The driving force for the crack extension in the x-direction can be readily obtained from eqn (12). The remaining problem is to seek the driving force for the deflection, or the stress intensity factors at the kink tip K_I^{tip} and K_{II}^{tip}.

As dictated by the linearity and dimensionality, the stress intensity factors at the kink tip must linearly depend on the remote ones. The solution is independent of kink size a, because it is the only length for the small-scale kink problem. Thus, all linearity coefficients depend only on the elastic parameters λ and ρ. A further simplification results from the

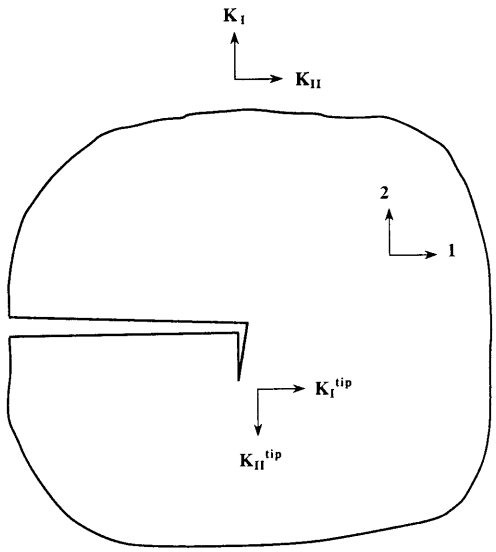

Fig. 4. Small-scale deflection in orthotropic materials. The remote loads and geometry are represented by the nominal stress intensity factors K_I and K_{II}. Stress itensity factors at the kink tip, K_I^{tip} and K_{II}^{tip}, are linearly dependent on the nominal stress intensity factors.

rescaling. As suggested by (10) and (11), the two pairs $(K_I^{tip}, \lambda^{-1/4}K_{II}^{tip})$ and $(\lambda^{-3/8}K_I, \lambda^{-1/8}K_{II})$ are related with coefficients depending on ρ only. Thus,

$$K_I^{tip} = c_{11}\lambda^{-3/8}K_I + c_{12}\lambda^{-1/8}K_{II}$$
$$K_{II}^{tip} = c_{21}\lambda^{-1/8}K_I + c_{22}\lambda^{+1/8}K_{II} \tag{27}$$

where $c_{ij} = c_{ij}(\rho)$ are functions of ρ only.

Values of the coefficients in Table 1 were calculated using an integral equation method described in Wang *et al.* (1991). Observe that these coefficients do vary to some extent within the practical range $0 < \rho < 4$, but the values for degenerate materials will be used

Table 1. Coefficients for small-scale kinking

ρ	c_{11}	c_{12}	c_{21}	c_{22}
0.1	0.397	1.073	−0.371	−0.216
0.3	0.390	1.104	−0.365	−0.210
0.5	0.384	1.132	−0.359	−0.204
0.7	0.379	1.158	−0.354	−0.200
0.9	0.375	1.182	−0.350	−0.196
1.1	0.369	1.204	−0.346	−0.193
1.6	0.360	1.255	−0.337	−0.185
2.1	0.352	1.299	−0.330	−0.178
2.6	0.345	1.339	−0.324	−0.173
3.1	0.338	1.375	−0.318	−0.168
3.6	0.333	1.409	−0.313	−0.164
4.1	0.328	1.439	−0.309	−0.160
4.6	0.323	1.468	−0.305	−0.157
5.1	0.319	1.495	−0.301	−0.154
5.6	0.315	1.521	−0.298	−0.151
6.1	0.311	1.545	−0.294	−0.148
6.6	0.308	1.569	−0.291	−0.146
7.1	0.305	1.591	−0.289	−0.144
7.6	0.302	1.612	−0.286	−0.142
8.1	0.299	1.632	−0.283	−0.140
8.6	0.296	1.652	−0.281	−0.138
9.1	0.294	1.671	−0.279	−0.136
9.6	0.292	1.689	−0.277	−0.135

in the following discussion for simplicity. The latter are identical to the isotropic solution of He and Hutchinson (1989):

$$c_{11} = 0.374, \quad c_{12} = 1.189, \quad c_{21} = -0.347, \quad c_{22} = -0.200, \quad \text{for } \rho = 1. \tag{27a}$$

The energy release rates for a virtual crack extension in the y-direction can be readily evaluated by combining (27) and (13).

Consider an important case when the parent crack is normal to the fiber direction, and the remote load is pure mode I. The driving force ratio of the deflection to straight extension is

$$G^{\text{tip}}/G_{\text{I}} = (c_{11}^2 + c_{21}^2)\lambda^{-1/4} = 0.260\lambda^{-1/4}. \tag{28}$$

The physical significance of the result may be appreciated as follows. Suppose the fracture energy for straight extension is Γ, and the fracture energy for the delamination in the fiber-containing plane is Γ_d. According to (28), deflection is favored as opposed to straight extension if

$$\Gamma_d/\Gamma < (c_{11}^2 + c_{21}^2)\lambda^{-1/4} = 0.260\lambda^{-1/4}. \tag{29}$$

Observe that elastic orthotropy ($\lambda > 1$) *lowers* the possibility of deflection, all other aspects being fixed. Notice that the delamination energy Γ_d usually depends on the relative proportion of sliding and opening measured by the loading phase $\psi = \tan^{-1}(|K_{\text{II}}^{\text{tip}}|/K_{\text{I}}^{\text{tip}})$. For the present situation as inferred from (27), Γ_d at loading phase $\psi = \tan^{-1}(\lambda^{1/4}|c_{21}|/c_{11}) = \tan^{-1}(0.928\lambda^{1/4})$ is the relevant quantity.

For both orientations of cracks in composites (i.e. both normal and parallel to the fibres) initial extension is likely to be parallel to the fibres by matrix cracking. Consider next the possible correlation of the macroscopic fracture toughnesses for cracks in the two orientations. Suppose the matrix cracking is a mode I controlled process which takes place when $G_{\text{I}}^{\text{tip}} = \Gamma_m$, where Γ_m is essentially the matrix fracture energy for brittle composites. The postulate is analogous to the one based on the hoop stress proposed by Ashby *et al.* (1985). With this postulate, eqn (27) predicts the nominal fracture energy Γ_∞ for pre-existing cracks normal to the fibers

$$\Gamma_\infty/\Gamma_m = \lambda^{1/4}/c_{11}^2 = 7.15\lambda^{1/4}. \tag{30}$$

The result indicates that elastic orthotropy ($\lambda \gg 1$) enhances the nominal fracture energy for pre-existing cracks normal to the fibers. It is important to notice that fracture normal to fibers in brittle composites is strongly resisted by fiber pull-out leading to resistance curves. The prediction (30) only gives the initiation fracture energy which should not be confused with the steady-state values.

As already emphasized, the relation (27) holds only when the kink size is small compared with all other macroscopic lengths. An intermediate-scale kinking model taking into account the in-plane stress (He *et al.*, 1990) can also be extended with the orthotropy rescaling. A large-scale delamination problem is discussed in the following section.

6. SURFACE FLAW INDUCED DELAMINATION

Laminates fabricated either with plies of carbon–epoxy composites or with alternate sheets of metals and ceramics exhibit several common features in the failure progression, such as cracks tunneling through the off-axis plies or the ceramic layers, and interfacial delamination. Delamination is also a dominant failure mode in uniaxially reinforced composites.

Attention here is focused on delamination induced by surface flaws in woods or uniaxially reinforced composites. Incipient delamination splits are not well characterized for two reasons. Under fixed nominal loads, firstly, the driving force at the crack tip depends

sensitively on the surface flaw geometry that induces the delamination. Secondly, the cracking is strongly resisted by the fiber cross-over or matrix ligament bridging that lead to resistance curves (de Charentenay *et al.*, 1984; Sbaizero *et al.*, 1990). Once the split is sufficiently long, however, the delamination attains a steady-state: both driving force and fracture resistance become independent of the split length and initial flaw geometry. A large-scale bridging model has been developed recently to account for the observed fracture resistance curves (Bao *et al.*, 1990; Suo *et al.*, 1990). To gain insight into the effects of anisotropy, here we will study the steady-state driving force and the transient zone size for a specific example, with bridging assumed not to occur.

A delamination crack originated from a notch under axial tension is depicted in Fig. 5a. The geometry is representative of a large family of beam-like specimens, such as crack-lap-shear (CLS) specimens, used by the composite materials community to study mixed-mode fracture, notch sensitivity and delamination. The energy release rates take the non-dimensional form

$$\frac{G_{\mathrm{I}}}{s_{11}\sigma^2 h} = g_{\mathrm{I}}\left(\lambda^{1/4}\frac{a}{h}, \frac{H}{h}, \rho\right), \quad \frac{G_{\mathrm{II}}}{s_{11}\sigma^2 h} = g_{\mathrm{II}}\left(\lambda^{1/4}\frac{a}{h}, \frac{H}{h}, \rho\right) \tag{31}$$

where the rescaling information has been built in. For the degenerate materials with $\rho = 1$, the results are identical to those for isotropic solids except for the rescaling. The latter solutions have been partially reported in Thouless *et al.* (1989) and Bao *et al.* (1990), and the more complete results are plotted in Fig. 5.

Observe that the energy release rate attains the steady-state when the split is sufficiently long. Inspection of Fig. 5b–d suggests that the *transient zone* size is roughly given by $\lambda^{1/4}a/h \approx 2$, or

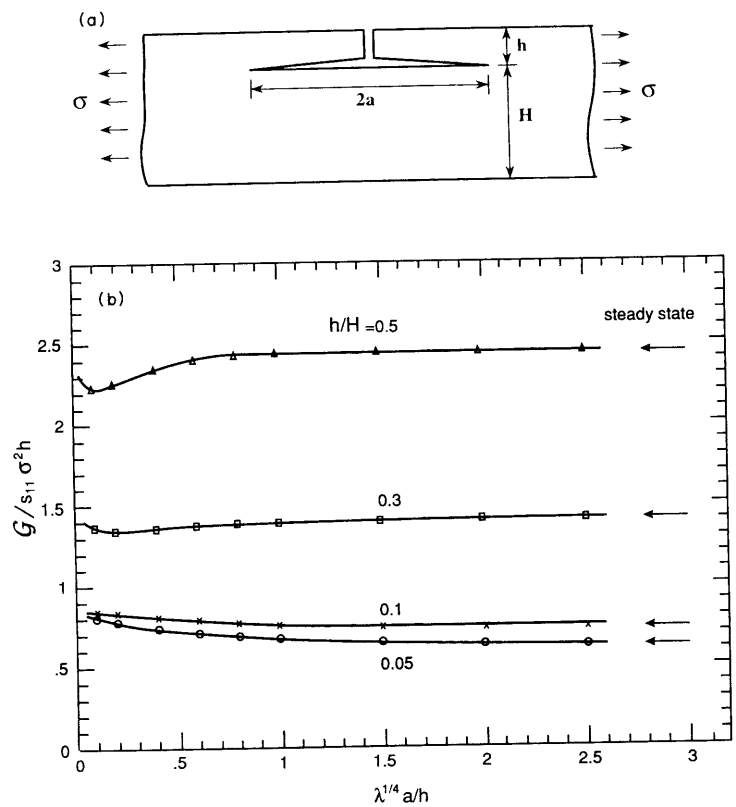

Fig. 5. (a) Delamination initiated from a notch and driven by the axial load. (b) The normalized total energy release rate. The interplay between orthotropy and delamination length is captured by the combination $\lambda^{1/4}a/h$. (c), (d) The mode I and mode II energy release rates.

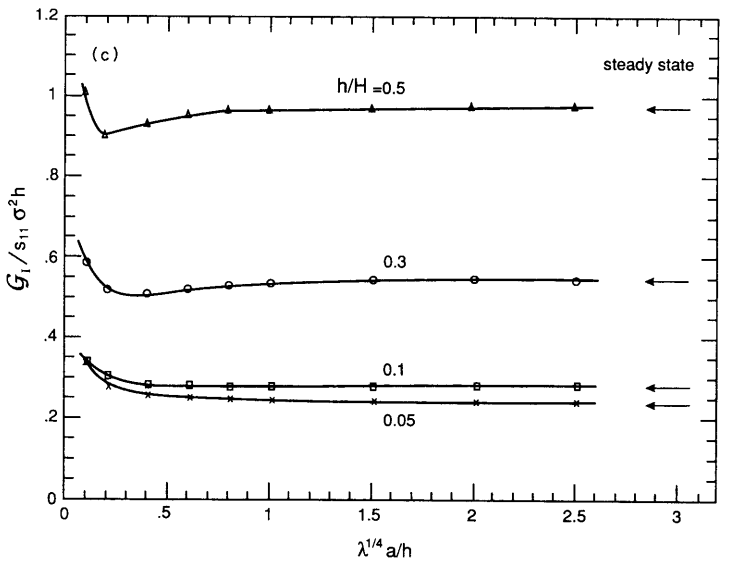

Fig. 5 (c)

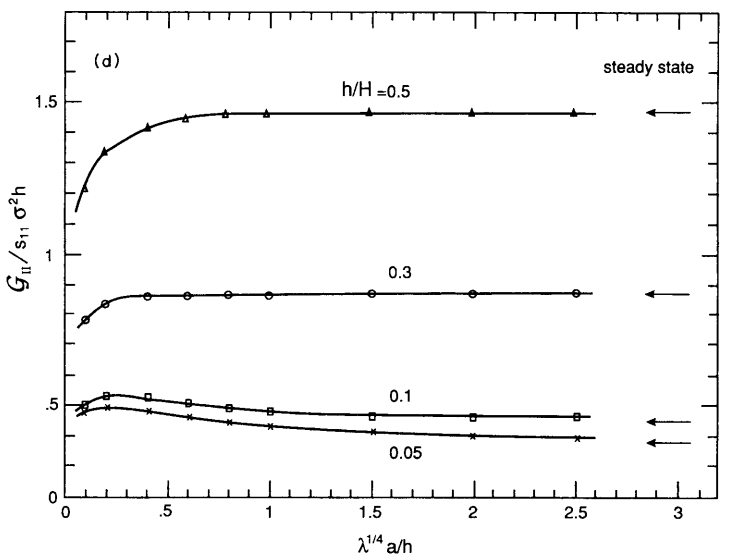

Fig. 5 (d)

$$a/h \approx 2\lambda^{-1/4}. \tag{32}$$

A split longer than a few times notch size is subjected to nearly constant driving force at a fixed nominal tensile stress. Equation (32) also reveals that elastic orthotropy tends to *prolong* the transient zone by a factor of $\lambda^{-1/4}$. The steady-state condition (32) is roughly valid for all beam-like specimens with the edges subjected to axial forces or bending moments without shear forces.

A finite element calculation has been made to study the ρ-effect in the transient zone. The results are plotted in Fig. 6. Apparently, the initial stage of the split is influenced by ρ to some extent, yet the size of the transient zone is not significantly modified so that eqn (32) remains valid for generally orthotropic materials.

Since the steady-state condition (32) can be easily satisfied in practice, the steady-state problems, a semi-infinite crack in an infinite strip, are therefore of particular significance. The problems have been solved *completely* for arbitrary edge loads in Suo (1990a). Specialized to the present edge load, the mode I and mode II energy release rates are

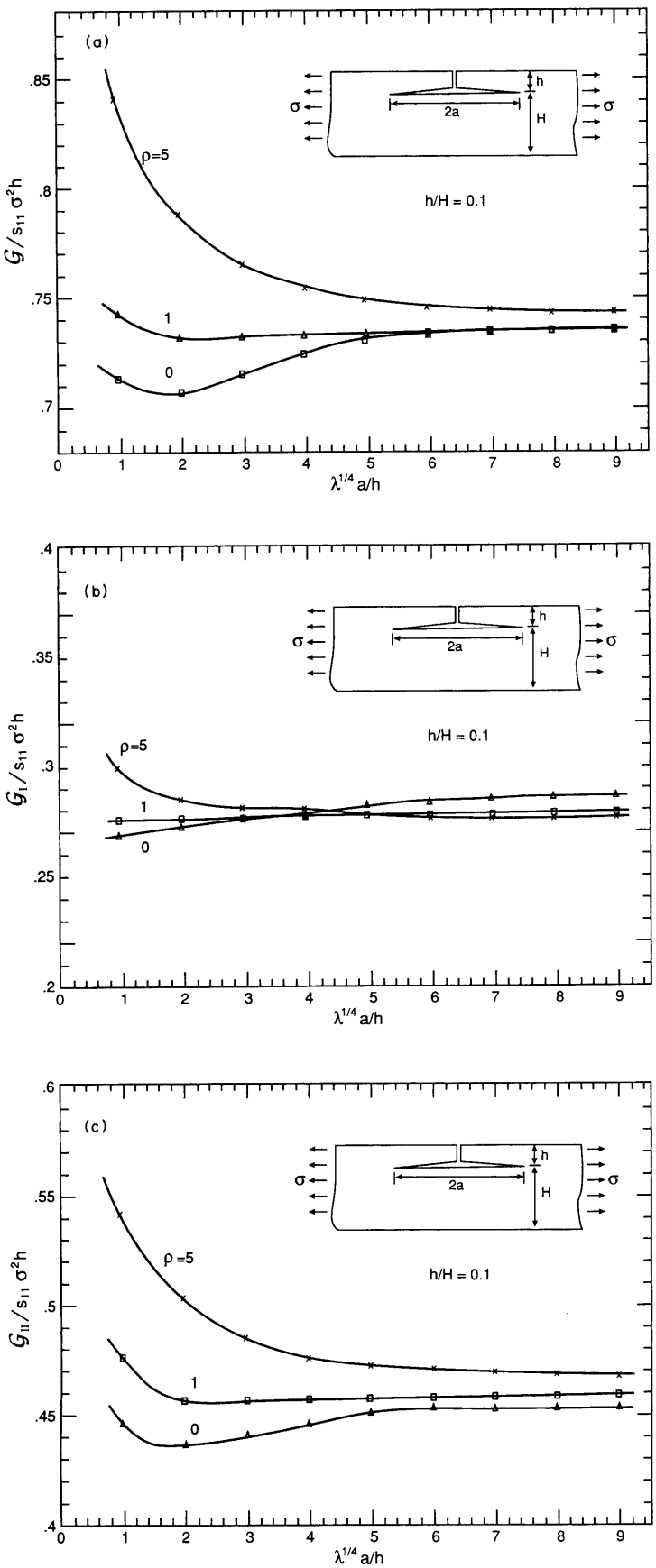

Fig. 6. The ρ dependence in the transient zone.

$$G_I/(s_{11}\sigma^2 h) = \tfrac{1}{2}(1+4\eta+6\eta^2+3\eta^3)\cos^2\omega$$
$$G_{II}/(s_{11}\sigma^2 h) = \tfrac{1}{2}(1+4\eta+6\eta^2+3\eta^3)\sin^2\omega \quad (33)$$

where $\eta = h/H$, and ω depends on η and ρ only but is independent of λ as a consequence of the orthotropy rescaling. Numerical calculations give

$$\omega \approx 52.1^0 - 3^0\eta. \quad (34)$$

The error of the above approximate formula is within 1% for the entire practical range $0 < \eta < 1$ and $0 < \rho < 5$. Notice that the normalized steady-state energy release rates are strictly independent of λ and approximately independent of ρ, and therefore approximately identical to those for isotropic solids. The conclusion remains valid for arbitrary edge loads; an important point that has not been appreciated in the earlier paper. The steady-state solution (33) is also included in Fig. 5.

The crack tip loading phase ψ, defined by $\tan\psi \equiv K_{II}/K_I$, is a measure of the proportion of the shear and tensile stresses ahead of the crack tip. Combination of (12) and (33) gives

$$\tan\psi = \lambda^{-1/4}\tan\omega. \quad (35)$$

Equations (34) and (35) suggest that the loading phase ψ does *not* vary much with the geometric ratio h/H, but can be substantially modified by the orthotropy. A larger shear component is anticipated for significant orthotropy ($\lambda < 1$).

7. CONCLUDING REMARKS

For traction-prescribed plane problems, the elastic orthotropy is characterized by two dimensionless parameters λ and ρ. The orthotropy rescaling transforms problems to equivalent ones for materials with cubic symmetry. We demonstrate that this idea, together with other elementary analytic considerations, simplifies a variety of problems of practical significance for unidirectional composites. For example, an accurate, simple calibration for double-cantilever beams is given by eqn (26). Many other specimens are compiled in the same way by Bao *et al.* (1991). Several limitations are observed. The method is useful only for load prescribed boundary conditions, since displacement boundary conditions would introduce additional material dependence. For problems with finite geometry, the rescaling changes the aspect ratio, so that it is advantageous only when the problems are analyzed systematically, with variable aspect ratios.

Acknowledgements—Funding for this work was supplied by the DARPA through the University Initiative Program of University of California at Santa Barbara under ONR contract No. N-0-0014-86-K-0753, and College of Engineering, UCSB. ZS is in addition supported by an NSF research initiative award (MSS-9011571). Table 1 was constructed when TCW was a visiting Professor at Brown University.

REFERENCES

Ashby, M. F., Easterling, K. E., Harrysson, R. and Maiti, S. K. (1985). The fracture and toughness of woods. *Proc. R. Soc. Lond* **398A,** 261–280.

Bao, G., Fan, B. and Evans, A. G. (1990). Mixed mode delamination cracking in brittle matrix composites. *Mech. Mater.* (in press).

Bao, G., Ho, S., Fan, B. and Suo, Z. (1991). The role of material orthotropy in fracture specimens for composites. Submitted to *Int. J. Solids Structures.*

de Charentenay, F. X., Harry, J. M., Prel, Y. J. and Benzeggagh, M. L. (1984). Characterizing the effect of delamination defect by mode I delamination test. *Effect of Defects in Composite Materials. ASTM STP* **836,** 84–103.

Evans, A. G. (1990). Perspective on the development of high-toughness ceramics. *J. Am. Ceram. Soc.* **73,** 187–206.

He, M.-Y. and Hutchinson, J. W. (1989). Kinking of a crack out of an interface. *J. Appl. Mech.* **56,** 270–278.

He, M.-Y., Bartlett, A., Evans, A. G. and Hutchinson, J. W. (1990). Kinking of a crack out of an interface: role of in-plane stress. *J. Am. Ceram. Soc.* (in press).

Lekhnitskii, S. G. (1981). *Theory of Elasticity of an Anisotropic Body.* Mir Publishers, Moscow.

O'Brien, T. K. (1987). Generic aspects of delamination in fatigue of composite materials. *J. Am. Helicopter Soc.* **32,** 13–18.

Peterson, R. E. (1974). *Stress Concentration Factors*. John Wiley, New York.
Sbaizero, O., Charalambides, P. G. and Evans, A. G. (1990). Delamination cracking in a laminated ceramic matrix composite. *J. Am. Ceram. Soc.* **73,** 1936–1940.
Sih, G. C., Paris, P. C. and Irwin, G. R. (1965). On cracks in rectilinearly anisotropic bodies. *Int. J. Fracture Mech.* **1,** 189–203.
Suo, Z. (1990a). Delamination specimens for orthotropic materials. *J. Appl. Mech.* **57,** 627–634.
Suo, Z. (1990b). Singularities, interfaces and cracks in dissimilar anisotropic media. *Proc. R. Soc. Lond.* **427A,** 331–358.
Suo, Z., Bao, G. and Fan, B. (1990). Delamination *R*-curve phenomena due to damage. *J. Mech. Phys. Solids* (in press).
Sweeney, J. (1988). The stress intensity for an edge crack in a semi-infinite orthotropic body. *Int. J. Fracture* **37,** 233–241.
Sweeney, J., Duckett, R. A. and Ward, I. M. (1988). The fracture behavior of oriented polyethylene at high pressure. *Proc. R. Soc. Lond.* **420A,** 53–80.
Tada, H., Paris, P. C. and Irwin, G. R. (1985). *The Stress Analysis of Cracks Handbook*. Del Research, St. Louis, MO.
Thouless, M. D., Cao, H. C. and Mataga, P. A. (1989). Delamination from surface cracks in composite materials. *J. Mater. Sci.* **24,** 1406–1412.
Wang, T. C., Shih, C. F. and Suo, Z. (1991). Crack extension and kinking in laminates and bicrystals. *Int. J. Solids Structures* (in press).
Wiederhorn, S. M., Shorband, A. M. and Moses, R. L. (1968). Critical analysis of the theory of the double cantilever method of measuring fracture surface energy. *J. Appl. Phys.* **39,** 1569–1572.

APPENDIX

Let the coordinates x, y and z coincide with principal material directions of an orthotropic solid. Hooke's law may be written as

$$\begin{Bmatrix} \varepsilon_x \\ \varepsilon_y \\ \varepsilon_z \\ \gamma_{yz} \\ \gamma_{zx} \\ \gamma_{xy} \end{Bmatrix} = \begin{bmatrix} s_{11} & s_{12} & s_{13} & 0 & 0 & 0 \\ s_{21} & s_{22} & s_{23} & 0 & 0 & 0 \\ s_{31} & s_{32} & s_{33} & 0 & 0 & 0 \\ 0 & 0 & 0 & s_{44} & 0 & 0 \\ 0 & 0 & 0 & 0 & s_{55} & 0 \\ 0 & 0 & 0 & 0 & 0 & s_{66} \end{bmatrix} \begin{Bmatrix} \sigma_x \\ \sigma_y \\ \sigma_z \\ \tau_{yz} \\ \tau_{zx} \\ \tau_{xy} \end{Bmatrix} \tag{A1}$$

where $s_{ij} = s_{ji}$ are compliances. For plane stress problems in the xy-plane, the relevant compliances that appear in the governing equation (5) of the text are s_{11}, s_{22}, s_{12} and s_{66}. For plane strain problems, the governing equation and the definition of λ and ρ remain unchanged except that all compliances need be replaced by (Lekhnitskii, 1981)

$$s'_{ij} = s_{ij} - s_{i3}s_{j3}/s_{33}. \tag{A2}$$

This replacement should be done with all the solutions in the text if the plane strain conditions prevail.